Energy gap and optical properties of InxGa1−xN

9 **AUTHORS**, INCLUDING:

F. Bechstedt
Friedrich Schiller University Jena
619 PUBLICATIONS **16,348** CITATIONS

SEE PROFILE

Jürgen Furthmüller
Friedrich Schiller University Jena
193 PUBLICATIONS **44,203** CITATIONS

SEE PROFILE

Lara K. Teles
Instituto Tecnologico de Aeronautica
63 PUBLICATIONS **1,015** CITATIONS

SEE PROFILE

Energy gap and optical properties of $In_xGa_{1-x}N$

F. Bechstedt[1,*], **J. Furthmüller**[1], **M. Ferhat**[1], **L. K. Teles**[2], **L. M. R. Scolfaro**[2], **J. R. Leite**[2], **V. Yu. Davydov**[3], **O. Ambacher**[4], and **R. Goldhahn**[5]

[1] Institut für Festkörpertheorie und Theoretische Optik, Friedrich-Schiller-Universität, Max-Wien-Platz 1, D-07743 Jena, Germany

[2] Instituto de Fisica, Universidade de São Paulo, CP66318, 05315-970 São Paulo, SP, Brazil

[3] Ioffe Physico-Technical Institute, Russian Academy of Science, Polytechnicheskaya 26, 194021 St. Petersburg, Russia

[4] Center for Micro- and Nanotechnologies, Technical University, P.O. Box 100565, 98693 Ilmenau, Germany

[5] Institut für Physik, Technische Universität Ilmenau, PF 100565, 98684 Ilmenau, Germany

We present *ab initio* calculations of the electronic structure and the optical properties of $In_xGa_{1-x}N$. They are completed by studies of the strain influence on the alloys. The results are critically discussed in the light of recent experiments. We find an energy gap of InN < 1 eV and a nonparabolic absorption edge. The strong variation of the alloy gap with the In molar fraction is described by a composition-dependent bowing parameter. The tendency of spinodal decomposition is suppressed by biaxial strain. Its extent depends on the realization of strain accommodation.

1. Introduction The recent developments in blue-green optoelectronics are essentially due to the high efficiency of luminescence from $In_xGa_{1-x}N$/GaN heterostructures with $x \lesssim 0.2$. Despite of their importance several properties of $In_xGa_{1-x}N$ alloys are not fully understood, in particular not for more In-rich systems with $x > 0.2$. Among them are the optical transition energies, their composition dependence, the influence of alloy fluctuations and spinodal decomposition, and the strain influence on composition dependence and decomposition.

The optical properties of InN crystals are poorly known, since the available growth techniques have not allowed to produce epitaxial layers of high quality. Interband absorption performed on thin InN films deposited by sputtering techniques [1] and metalorganic vapour phase epitaxy (MOVPE) [2] were interpreted as being consistent with a fundamental energy gap of about 2 eV. No band-to-band photoluminescence (PL) could be observed, also not on InN layers grown by molecular beam epitaxy (MBE) [3]. The *ab initio* electronic-structure theory as a combination of the density functional theory (DFT) in local density approximation (LDA) and the quasiparticle theory taking the exchange-correlation self-energy in GW approximation into account [4] could not be used to predict a plausible gap value. Usually the DFT-LDA, in particular using pseudopotentials, gives an overlap of conduction and valence band states, i.e., a negative gap [5, 6]. Recent improvements in MBE have however led to the availability of InN films, which allow absorption, PL and photoluminescence excitation (PLE) spectroscopy measurements. These measurements indicate an energy gap of about 1 eV or less [7].

---

* Corresponding author: e-mail: bechstedt@ifto.physik.uni-jena.de

Measurements of the band gap of $In_xGa_{1-x}N$ found a strong variation with the composition for In molar fractions $x \lesssim 0.3$. The derived bowing parameter is however still a subject of a controversial discussion. Its measured values vary from 1 to 5 eV. With 1 . . . 2 eV the calculated bowing parameters are generally smaller [8]. In the intermediate range of compositions the $In_xGa_{1-x}N$ system shows a tendency for spinodal decomposition into two different random alloys [9]. However, this tendency is influenced by the strain state [10]. Assuming that in a coherently grown system the biaxially strain accommodation happens locally, complete suppression of decomposition is expected [11].

2. Computational methods   The calculations are based on the DFT in the LDA. We use a plane-wave expansion of the eigenfunctions and non-normconserving pseudopotentials implemented in the Vienna Ab initio Simulation Package (VASP) [12]. The Ga3d and In4d electrons are treated as valence electrons (*dval*). This guarantees correct structural properties of the $In_xGa_{1-x}N$ systems. The use of ultrasoft pseudopotentials allows a remarkable reduction of the plane-wave cutoff to 16.2 Ry. This DFT-LDA procedure, however, gives a negative fundamental energy gap for InN [5]. In the case of the solid-state calculations of the electronic structure and the optical properties of InN, we therefore also use another type of pseudopotentials which account for self-interaction corrections (SIC) of the 4d electrons in the underlying atomic calculation but freeze the In4d electrons in the core [13]. In order to account for the excitation aspect, quasiparticle (QP) corrections are taken into consideration [4]. The independent-particle approximation and the projector-augmented-wave (PAW) method [14] are applied to calculate complete optical spectra.

In order to describe the random $In_xGa_{1-x}N$ alloys we follow the cluster expansion approach (CEA) and the generalized quasichemical approximation (GQCA). Configurationally averaged quantities are calculated using the Conolly–Williams method. Clusters corresponding to 8-atom $In_nGa_{4-n}N_4$ and 64 atom $In_nGa_{32-n}N_{32}$ supercells are studied. The larger clusters allow a more precise description of the electronic properties, although not all atomic configurations can be included in the alloy statistics. The details of the procedure are described in Ref. [9]. The effect of a biaxial strain is modelled by fixing the lattice constants of the clusters with a certain composition parallel to the substrate [10].

3. Results
3.1 Electronic structure of InN   The structural parameters of wurtzite InN are calculated by minimizing the total energy. The inclusion of the In4d electrons allows the calculation of lattice constants $c = 5.688$ Å and $a = 3.523$ Å only slightly smaller than the experimental values [1, 7]. The underestimate of the lattice constants is a consequence of the overbinding tendency within the DFT-LDA. Unfortunately, the conduction and valence bands overlap around the Γ point in the Brillouin zone (BZ) resulting in a negative fundamental energy gap $E_g(dval) = -0.19$ eV. The same effect has been
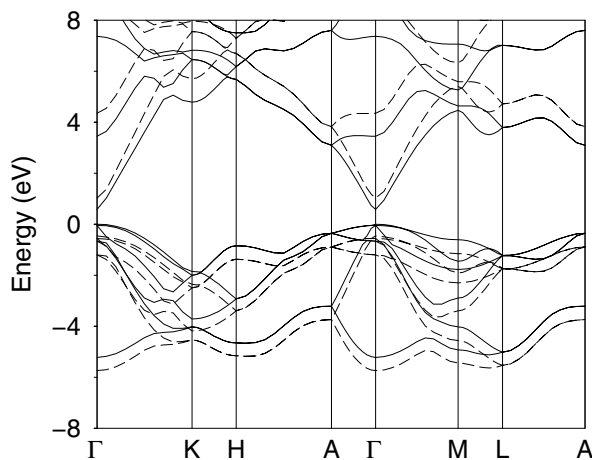

Fig. 1 Energy band structure of wurtzite InN. Solid lines: DFT-LDA, dashed lines: including quasiparticle corrections.

observed by other authors despite the inclusion of generalized gradient corrections to the exchange-correlation potential [6]. This overlap is mainly a consequence of the overestimation of the *pd* repulsion within DFT-LDA [15]. The In4*d* levels in the valence bands lie only 13.5 eV below the valence band maximum (VBM).

To avoid the overestimation of the *pd* repulsion we have also performed calculations where the In4*d* electrons are frozen in the core. The effect of these electrons is however considered constructing the pseudopotentials. A self-interaction correction (SIC) is taken into account [13]. The electronic-structure calculations at the theoretical lattice constants result in a band structure shown in Fig. 1. The fundamental gap is opened to $E_g(SIC) = 0.58$ eV. The $\Gamma_6 - \Gamma_1$ crystal-field splitting, $\Delta_{cr} = 15$ (dval) or 43 (SIC) meV, is positive. The SIC bands possess the correct energetical ordering. Their wave functions are completed to all-electron ones within the PAW procedure [14].

The resulting wave functions allow the calculation of the quasiparticle (QP) shifts and, hence, the QP band structure also shown in Fig. 1. In their calculation a computed average electronic dielectric constant of $\varepsilon_\infty = 7.16$ is used. The QP correction of the fundamental energy gap amounts $\Delta^{QP} = 0.93$ eV. This value is similar to those values 1.03 eV [16] and 0.80 eV [5] estimated by means of the Bech-stedt–Del Sole formula [17]. The resulting QP gaps are $E_g^{QP}(dval) = 0.74$ eV and $E_g^{QP}(SIC) = 1.50$ eV. The gap variation of 0.76 eV represents the total *pd* repulsion. Its true percentage contribution may be estimated from the true position of the In4*d* levels 14.9 eV below VBM [18]. Using perturbation-theory arguments and the DFT-LDA value of 13.5 eV, a fraction 13.5/14.9 should be involved. This allows the prediction of the true QP gap of $E_g = 0.81$ eV in-between $E_g^{QP}(dval)$ and $E_g^{QP}(SIC)$. The same procedure gives for zinc-blende InN the values $E_g(dval) = -0.36$ eV, $E_g(SIC) = 0.43$ eV, $\Delta^{QP} = 0.87$ eV, and $E_g = 0.58$ eV. There is also another measurement 16.7 eV for the distance In4*d*-VBM [19]. This gives a slightly larger gap value of 0.89 (0.67) eV for wurtzite (zinc-blende) InN. The gap of the cubic polytype is by about 0.2 eV smaller than that of the wurtzite structure. Meanwhile, experimentally a band gap of hexagonal InN in the range of 0.75 to 0.90 eV has been widely confirmed by transmission, PL and PLE studies [7].

3.2 Optical properties of InN The frequency-dependent dielectric function of wurtzite InN calculated within the approximation of In4*d* electrons frozen in the core, projector-augmented waves and independent particles is shown in Fig. 2. For comparison with experimental data [20] the spectra have to be shifted to higher energy by about 0.24 eV to account correctly for quasiparticle effects and *pd* repulsion. The resulting line shapes are similar to those obtained in previous calculations [16] as well as for GaN [21].
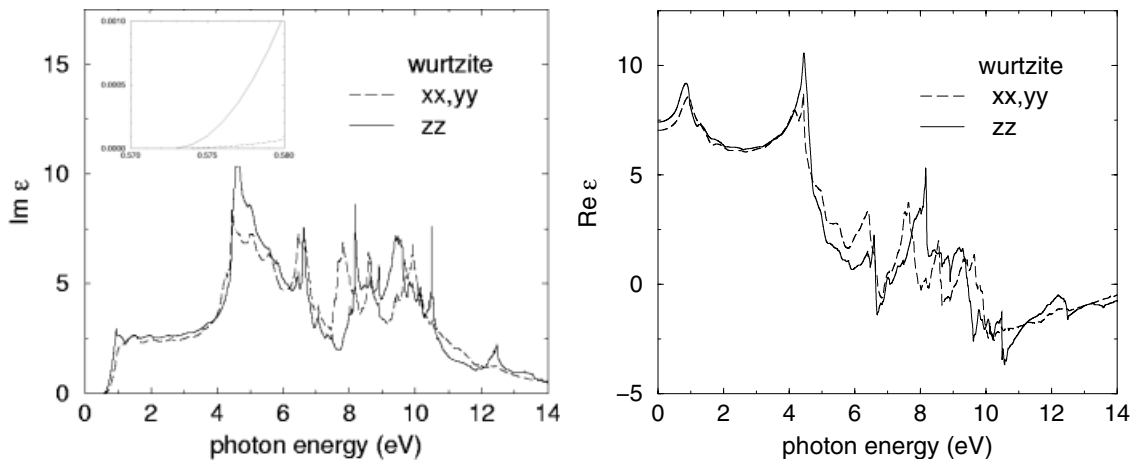

Fig. 2 Imaginary part (a) and real part (b) of the dielectric function of wurtzite InN. Light polarizations parallel (solid line) and perpendicular (dashed line) to the *c*-axis are considered.
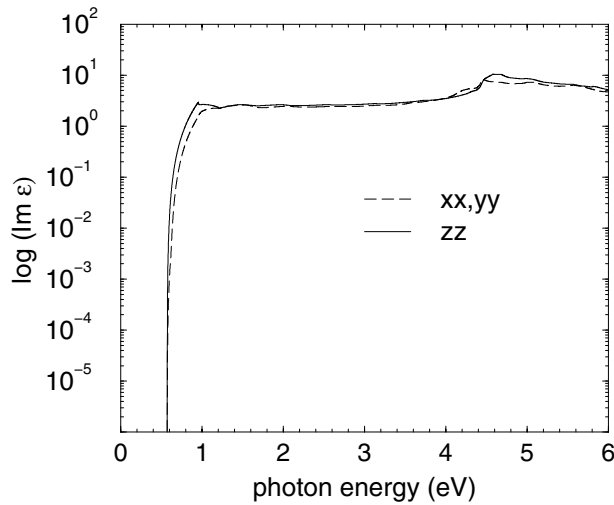
Fig. 3 Logarithmic representation of the absorption coefficient.

The behaviour of the optical absorption is most interesting. It shows a sharp onset, which is followed by a plateau. This deviation from the expected square-root dependence may be interpreted as a spectral feature indicating a strong nonparabolic character of the contributing bands. This character is more obvious in the logarithmic representation in Fig. 3. Similar spectra have been derived from ellipsometric and photothermal-deflection measurements. They clearly indicate a band gap below 1 eV. Only two pronounced spectral features appear near $\hbar\omega = 0.9$ eV and $\hbar\omega = 4.6$ eV (unrenormalized). The first structure should be a consequence of optical transitions near the Γ point. The second structure can be traced back to strong transitions between the highest valence and lowest conduction bands on the LM line in the hexgonal BZ (cf. Fig. 1).

3.3 Gap bowing in $In_xGa_{1-x}N$ Data for the energy gap of hexagonal $In_xGa_{1-x}N$ alloys are summarized in Fig. 4. They are mainly derived using PL. While many data exist for In molar fractions $x < 0.4$, the majority of gaps for alloys with $0.5 < x < 1.0$ has been measured recently on PAMBE and MOMBE samples [25]. The measurements of these values are influenced by a variety of effects, such as spinodal decomposition, alloy fluctuations, strain, chosen gaps of GaN and InN, and measurement technique. Nevertheless, Fig. 4 indicates a remarkable dependence of the gap on the composition and, hence, a considerable bowing. Using a conventional picture of the x-dependence of the gap, $E_g(x) = (1 - x) E_g(\text{GaN}) + x E_g(\text{In N}) - bx(1 - x)$, an average bowing parameter of about $b = 2.5$ eV follows [25]. In the $In_xGa_{1-x}N$ system the bowing is however not constant but itself composition-dependent. One finds roughly $b(x) = (1 - x) [11.4 - 19.4x]$ eV, i.e., $b(0.25) = 4.9$, $b(0.5) = 0.9$, and $b(0.75) = -0.8$ eV. As a consequence, the so-called bowing parameter depends on the composition interval considered.
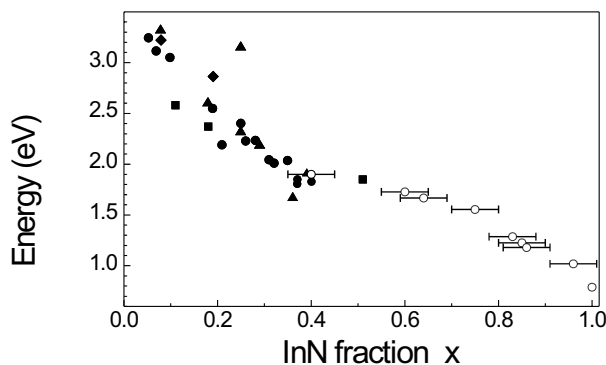

Fig. 4 Selected experimental data for the energy gap of $In_xGa_{1-x}N$ alloys. Filled circles and triangles: [22], filled squares: [23], filled diamonds: [24], and open circles: [25].

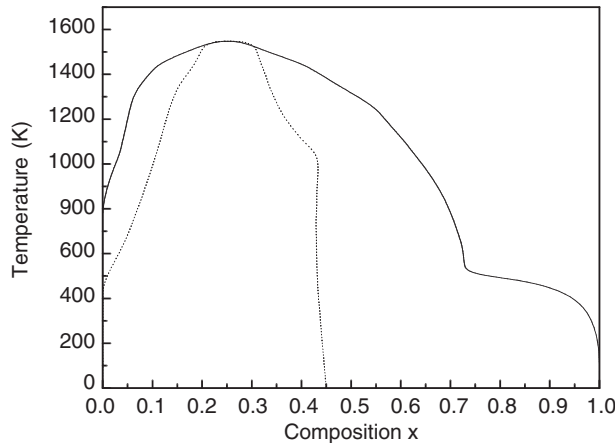**Fig. 5** $T - x$ phase diagram of strained In$_x$Ga$_{1-x}$N ternary alloy system. Pseudomorphic growth on GaN and global equlibrium are assumed. Solid line: binodal curve, dotted line: spinodal curve.

Not only the procedure to derive the band-gap bowing parameter from experimental data contains uncertainties but also the determination of the theoretical value depends on many details of the calculation, the alloy description, the cluster size, and the definition of the alloy gap [8–10, 26]. Considering large 64-atom clusters and the cubic polytype we indeed found a composition-dependent bowing, however, the absolute values are smaller than discussed above [8]. Within the interval $0 \le x \le 0.25$ the calculated values vary between 2.5 and 1.5 eV. For higher In molar fractions the b parameter decreases further to $b(0.5) = 1.4$ eV and $b(0.75) = 1.3$ eV. The main contribution to the bowing is due to a structural effect, the composition-induced disorder in the bond lengths [27]. This holds for the configurationally averaged gap. Studying other gaps, e.g. $E_{\mathrm{g}}(x) - \Delta E_{\mathrm{g}}(x)$ (which may be measured more or less in PL) with $\Delta E_{\mathrm{g}}(x)$ as the rms deviations, larger bowing parameters are extracted [9].

3.4 Strain influence on miscibility   The alloy properties, especially its optical properties, can be strongly influenced by a biaxial strain. This holds in particular for the composition region of the immiscibility gap in the thermodynamical equilibrium [9]. Usually a complete suppression of the spinodal decomposition is expected [10]. This effect has been indeed observed for cubic In$_x$Ga$_{1-x}$N [11]. However, changing only slightly the preparation procedure, the tendency for spinodal composition seems to be not suppressed [28].

In order to understand these contradicting experimental findings, we have recalculated the mixing free energy of the alloy within CEA and GQCA and tried to construct a $T - x$ phase diagram. The coherently strained alloys are modelled in two different ways. In both of them, the situation that each individual clusters is coherently strained is described by fixing its lattice constant parallel to the substrate. But in the first, the corresponding perpendicular lattice constant is minimized for each individual cluster. In this case, which can be viewed as the realization of a local equilibrium, the mixing free energy shows only one minimum. The miscibility gap vanishes [9]. And in the second, the minimum free energy is determined by varying the corresponding average perpendicular lattice constant of the whole alloy. This can be interpreted as a global equilibrium. The phase diagram resulting for pseudomorphic growth on a GaN substrate [28] is plotted in Fig. 5. The tendency for phase separation is reduced but not completely suppressed. This holds in particular for alloys with $x > 0.5$. Spontaneous decomposition cannot anymore be predicted for this composition range.

4. Summary   Combining DFT-LDA and quasiparticle shifts the ab initio theory predicts a fundamental energy gap for wurtzite InN slightly smaller than 1 eV. The exact value depends on the amount of pd repulsion and, hence, on the energetical distance of the valence band maximum and the In$4d$ levels in excitation spectroscopies. The absorption edge of InN shows a clear nonparabolic behaviour. The theoretical results are supported by recent optical measurements.

A central quantity to characterize the optical properties of $In_xGa_{1-x}N$ alloys is the fundamental energy gap. Despite of the difficulties with its exact definition, we predict a relatively strong and, in particular, composition-dependent bowing of the gap. It is mainly due to a structural effect related to the bimodal distribution of the bond lengths. Optical properties of alloys are also influenced by the tendency of spontaneous spinodal decomposition. This tendency is suppressed for biaxially strained layers. The suppression depends itself on the realization, in particular on the characteristic length scale, of the strain accommodation in the alloy.

References

[1]   T. L. Tansley and C. P. Foley, J. Appl. Phys. **59**, 3241 (1986).
[2]   Q. Guo and A. Yoshida, Jpn. J. Appl. Phys. **33**, 2453 (1994).
[3]   A. Tabata, A. P. Lima, L. K. Teles, L. M. R. Scolfaro, J. R. Leite, V. Lemos, B. Schöttker, T. Frey, D. Schikora, and K. Lischka, Appl. Phys. Lett. **74**, 362 (1999).
[4]   B. Wenzien, G. Cappellini, and F. Bechstedt, Phys. Rev. B **51**, 14701 (1995).
[5]   U. Grossner, J. Furthmüller, and F. Bechstedt, Phys. Rev. B **58**, R1722 (1998).
[6]   C. Stampfl and C. G. Van de Walle, Phys. Rev. B **59**, 5529 (1999).
[7]   V. Yu. Davydov, A. A. Klochikhin, R. P. Seisyan, V. V. Emtsev, S. V. Ivanov, F. Bechstedt, J. Furthmüller, H. Harima, A. V. Mudryi, J. Aderhold, O. Semchinova, and J. Graul, phys. stat. sol. (b) **229**, R1 (2002).
[8]   M. Ferhat, J. Furthmüller, and F. Bechstedt, Appl. Phys. Lett. **80**, 1394 (2002).
[9]   L. K. Teles, J. Furthmüller, L. M. R. Scolfaro, J. R. Leite, and F. Bechstedt, Phys. Rev. B **62**, 2475 (2000).
[10] L. K. Teles, J. Furthmüller, L. M. R. Scolfaro, J. R. Leite, and F. Bechstedt, Phys. Rev. B **63**, 085204 (2001).
[11] A. Tabata, L. K. Teles, L. M. R. Scolfaro, J. R. Leite, T. Frey, A. Kharchenko, D. J. As, D. Schikora, K. Lischka, J. Furthmüller, and F. Bechstedt, Appl. Phys. Lett. **88**, 769 (2002).
[12] G. Kresse and J. Furthmüller, Comput. Mater. Sci. **6**, 15 (1996); Phys. Rev. B **54**, 11169 (1996).
[13] M. M. Rieger and P. Vogl, Phys. Rev. B **52**, 16567 (1995).
[14] B. Adolph, J. Furthmüller, and F. Bechstedt, Phys. Rev. B **63**, 125108 (2001).
[15] F. Bechstedt, in Low-dimensional nitride semiconductors, ed. by B. Gil (Oxford University Press, Oxford 2002), p. 11.
        F. Bechstedt and J. Furthmüller, J. Cryst. Growth **246**, 315 (2002)
[16] C. Persson, R. Ahuja, A. Ferreira da Silva, and B. Johansson, J. Phys.: Condens. Matter **13**, 8945 (2001).
[17] F. Bechstedt and R. Del Sole, Phys. Rev. B **38**, 7710 (1988).
[18] Q. X. Guo, M. Nishio, H. Ogawa, A. Wakahara, and A. Yoshida, Phys. Rev. B **58**, 15304 (1998).
[19] Y. Bu, L. Ma, and M.C. Lin, J. Vac. Sci. Technol. A **11**, 2931 (1993).
[20] Q. Guo, O. Kato, M. Fujisawa, and A. Yoshida, Solid State Commun. **83**, 721 (1997).
[21] W. R. L. Lambrecht and M. Prikhodko, Solid State Commun. **121**, 549 (2002).
[22] K. P. O'Donnell, Mat. Res. Soc. Symp. **595**, W11.26.1 (2000).
[23] M. Kim, J.-K. Cho, I.-H. Lee, S.-J. Park, phys. stat. sol. (a) **176**, 269 (1999).
[24] W. Shan, B. D. Little, J. J. Song, Z. C. Feng, M. Schurman, and R. A. Stall, Appl. Phys. Lett. **69**, 3315 (1996).
[25] V. Yu. Davydov, A. A. Klochikhin, V. V. Emtsev, S. V. Ivanov, V. V. Vekshin, F. Bechstedt, J. Furthmüller, H. Harima, A. V. Mudryi, A. Hashimoto, Y. Yamamoto, J. Aderhold, J. Graul, and E. E. Haller, phys. stat. sol. (b) **230**, R4 (2002); unpublished.
[26] W. R. L. Lambrecht, Solid State Electron. **41**, 195 (1997).
[27] M. Ferhat and F. Bechstedt, Phys. Rev. B **65**, 075213 (2002).
[28] L. K. Teles, J. Furthmüller, L. M. R. Scolfaro, D. J. As, D. Schikora, K. Lischka, F. Bechstedt, and J. R. Leite, unpublished.